

# An EEG-based approach for Parkinson's disease diagnosis using capsule network

Shujie Wang<sup>1,a</sup>, Gongshu Wang<sup>1</sup>, Guangying Pei<sup>1,b</sup>

<sup>1</sup>School of Life Science, Beijing Institute of Technology, Haidian District, Beijing, China

<sup>a</sup>wangshujie@bit.edu.cn

<sup>b</sup>pei\_guangying@bit.edu.cn

**Abstract**—As the second most common neurodegenerative disease, Parkinson's disease has caused serious problems worldwide. However, the cause and mechanism of PD are not clear, and no systematic early diagnosis and treatment of PD have been established. Many patients with PD have not been diagnosed or misdiagnosed. In this paper, we proposed an EEG-based approach to diagnosing Parkinson's disease. It mapped the frequency band energy of electroencephalogram(EEG) signals to 2-dimensional images using the interpolation method and identified classification using capsule network(CapsNet) and achieved 89.34% classification accuracy for short-term EEG sections. A comparison of separate classification accuracy across different EEG bands revealed the highest accuracy in the gamma bands, suggesting that we need to pay more attention to the changes in gamma band changes in the early stages of PD.

**Keywords**—Parkinson's disease; machine learning; deep learning; electroencephalograph; capsule network

## I. INTRODUCTION

Parkinson's disease (PD) is the second most common neurodegenerative disease worldwide, frequently in the elderly and affecting 2% – 3% of people over 60[1,2]. According to the global burden of disease study, neurological diseases are currently the major source of disability worldwide, and PD is the fastest growing disease of these diseases (with age-standardized prevalence, disability and mortality). From 1990 to 2015, the number of people with Parkinson's disease worldwide increased by 118% to 6.2 million [3,4].

The main clinical manifestations of PD include delay, limb stiffness, static tremor and gait disorder; in many patients, sleep disorders and anxiety are present. To date, there are no effective treatment means, mainly relying on drug intervention and comprehensive treatment to delay the progress of the disease, but the efficacy of drugs in the middle and late stages gradually decline, and complications gradually appear. Although surgical treatment can be used as a means of middle and late PD treatment, limited clinical application is applied due to invasive treatment and high cost [5]. Therefore, the early diagnosis of PD is particularly important.

However, the cause and mechanism of PD are not clear, and no systematic early diagnosis and treatment of PD have been established. Many patients with PD are not diagnosed or misdiagnosed, resulting in a large number of actual PD patients being unable to receive the corresponding treatment [6]. The difficulty in early diagnosis of PD is the inconspicuous

characteristics and susceptibility to confusion with other diseases[7]. Therefore, how to effectively extract the features in the input signal and then improve the Parkinson's disease diagnosis accuracy is an important difficulty in PD diagnosis.

Electroencephalogram (EEG) can record the spontaneous, rhythmic electrical activity of brain cells with good temporal resolution, is relatively easy to collect and is widely used in the detection of neurological diseases. Studies show that the most important EEG change in PD patients is the main wave frequency (dominant frequency, DF) from rhythm to slower high rhythm, namely, EEG slows down [8]. EEG can be used for the detection of nonmotor symptoms, such as EEG studies in PD patients with depressive symptoms showing increased wave and wave activity [9]. PD motor symptoms are closely related to the frequency band, and continuous motor task completion is related to a specific EEG frequency band, including frequency bands corresponding to movement preparation, movement control and execution of the corresponding frequency band and conflict signal processing [10-13]. As the main rhythm in the cortical-spinal system, frequency bands are important in coordinating motor function, and motor abnormalities in PD may cause [14,15] increased high-frequency coherence in the mesomotor cortical-subcortical region. Combined, past studies have found that EEG can more objectively and quantitatively represent the disease process and symptoms of PD patients, which can effectively guide the early diagnosis of PD[16-18]. Among these models, convolutional neural networks (CNNs) have shown superiority in physiological signal recognition[19]. However, the pooling layer in CNN ignores much information because of its data compression functions and static routing, and a capsule network (CapsNet) can solve this problem[20]. CapsNet considers the spatial relationships between features, simulates the human brain learning process, and achieves the best results on the MNIST dataset.

Table. 1 Demographic data.

	PD	HC	P value
N (sex ratio M/F)	55 (29/26)	30 (15/15)	0.813
Age (SD), year	59.82 (7.33)	57.73 (7.63)	0.226
MMSE (SD)	27.35 (1.71)	27.53 (2.50)	0.888
Education (SD), year	4.24 (0.94)	3.9 (1.22)	0.198
UPDRS III (SD)	30.42 (12.52)	-	-
MoCA (SD)	25.52 (3.27)	-	-
H&Y (SD)	2.25 (0.49)	-	-

UPDRS III, Movement Disorders Society-Unified Parkinson’s Disease Rating Scale-Part III; MoCA, Beijing version of the Montreal Cognitive Assessment; H&Y, Hoehn & Yahr stage;

In this paper, we propose an EEG-based approach for Parkinson’s disease diagnosis with a capsule network. First, we project the energy features of the different frequency bands of the EEG to the corresponding spatial positions by the interpolation method to construct the EEG map of the different frequency bands, in which the raw signals of EEG are converted to 2D images, and then enter the EEG maps into CapsNet for training and testing. To the best of our knowledge, this is the first attempt to diagnose Parkinson’s disease with a capsule network.

## II Materials and Methods

### A. Participants

Eighty-five participants were recruited from November 2019 to January 2021 in the present study. Fifty-five nondemented Parkinson’s disease patients were recruited from the Neurological Rehabilitation Center of Beijing Rehabilitation Hospital Affiliated to Capital Medical University, and 30 healthy controls were recruited by the local community recruiting ads. Demographic and clinical details are summarized in Table 1. This study was approved by the Ethics Committee of the Beijing Rehabilitation Hospital Affiliated with Capital Medical University and Aerospace Central Hospital following the Declaration of Helsinki, and all participants provided informed written consent before the experiment.

### B. EEG data collection and processing

Using the BP Company 32 Guide EEG Acquisition Equipment (Brain products, Germany) for EEG data acquisition, EEG acquisition was based on the International 10/20 system. EEG was collected from 30 channels (FP1, FP2, F7, F3, Fz, F4, F8, T3, C3, Cz, C4, T4, T5, P3, Pz, P4, T, T6, FT9, FC5, FC1, CP5, CP1, Oz, CP6, CP2, FT10, FC6, FC2, O1 and O2). The reference electrode was set as the left and right papillary electrodes (TP9, TP10). The grounding electrode was placed in front of it. The sampling rate was 1,000 Hz. The scalp impedance was reduced to 5 k $\Omega$  at the acquisition. Eye-open and closed resting EEG signals were collected simultaneously for each subject for 15 min each.

EEG signal preprocessing mainly includes the following steps: data preview, electrode positioning, filtering, independent component analysis (ICA), artifact deletion, and segmentation. First, a double electrode reference was used to reduce the error and brain hemisphere effect caused by the single reference electrode. Second, filtering the data from the high-frequency band and working frequency interference baseline drift by 0.5 Hz high-pass and 45 Hz low-frequency FIR filter. Third, ICA is used to remove noise components such as EMG and EMO to obtain relatively pure EEG signals. Finally, the preprocessed EEG data were split into 5 s + 5 s epochs (open + close). To ensure that the number of epochs was the same between subjects, 90 valid epochs without artifacts were selected from each PD subject, and 165 valid epochs without artifacts were selected from each HC subject. Therefore, we obtained 4950 epochs for the PD group and 4950 epochs for the HC group, 9900 epochs in total.

Considering the inherent structure of the data in space, frequency, and time, we used a method proposed by Pouya Bashivan et al. to transform the measurements into a 2-D image to save the spatial structure and used multiple color channels to represent the spectral dimension[21]. As shown in figure.1, for each epoch of EEG data, the energy features of theta (4-8 Hz), alpha (8-13 Hz), beta (13-30 Hz), and gamma (30-45 Hz) frequency bands in each channel were calculated by the Welch method, and the electrode 3 D coordinates were extracted from the equipment information. Azimuthal equidistant projection (AEP) was used to project the electrode position to the 2 D plane. Finally, the scattering power measurement on the scalp was interpolated for an EEG feature image of 8 (four band energy characteristics and two eye-open states) $\times 32 \times 32$  (32 $\times 32$  grid). Thus, the topographic features of the EEG spectrum energy were retained, which was more conducive to the input of the subsequent deep learning model. Finally, for k-fold cross validation, we randomly divided each group of EEG feature images into five parts, and each part of the data contained data from 6 HC individuals and 11 PD individuals.

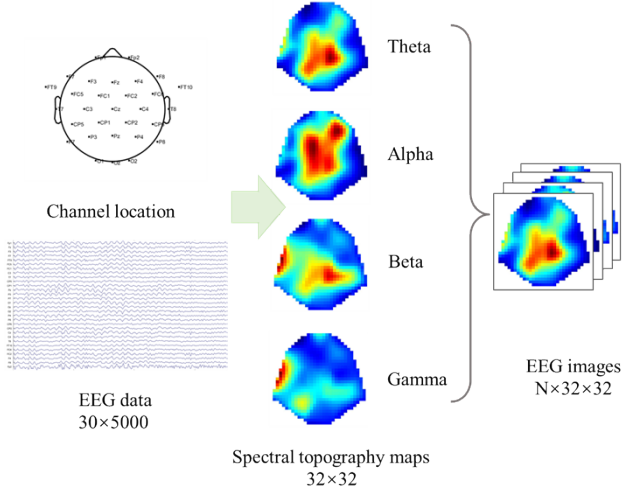


Figure 1. The method to generate 2d EEG images from EEG data

### C. CapsNet

Capsule network is a neural network instead of scalar neurons of a convolutional neural network (CNN), which can better capture and characterize the relationship between the characteristic attributes of the input signal (such as relative location, scale, direction, etc). The CapsNet model retains the convolutional properties of the convolutional neural network, creates higher-level capsules to cover a larger region of the image, and does not lose the exact location information within the region, while combining the capsules with dynamic routing, improving the efficiency of the capsule network.

Unlike the scalar neurons in the convolutional neural network, capsule  $j$  (vector neuron  $j$ ) in the capsule network uses a matrix  $W_{ij}$  to process the input vector  $u_i$  into new input vectors  $\hat{u}_{j|i}$ , as shown in (1).

$$\hat{u}_{j|i} = W_{ij} u_i \quad (1)$$

The input vector  $\hat{u}_{j|i}$  is then multiplied by the weight  $c_{ij}$ , and the total input of capsule  $j$  is obtained after the sum of the weighted vector, as shown in (2).

$$s_j = \sum_i c_{ij} \hat{u}_{j|i} \quad (2)$$

Using a nonlinear "squashing" function as activation to ensure that the capsule output vector  $v_j$  is between 0-1,  $v_j$  could represent the probability that the entity represented by the capsule is present in the current input, as shown in (3).

$$v_j = \frac{\|s_j\|^2 s_j}{1 + \|b_j\|^2 + \|s_j\|^2} \quad (3)$$

The weight  $c_{ij}$  in (2) is the coupling coefficient determined by the iterative dynamic routing process. The sum of the coupling coefficient between all  $k$  capsules of capsule  $i$  and the upper layer is 1.  $c_{ij}$  is decided by the "Routing softmax", as shown in (4).

$$c_{ij} = \frac{\exp(b_{ij})}{\sum_k \exp(b_{ik})} \quad (4)$$

In formula (3),  $b_{ij}$  is the log-prior probability that capsule  $i$  should be coupled to capsule  $j$ .  $b_{ij}$  obtained by distinction learning, as with all other weights, depends on the location and type of the two capsules rather than the current input. For the first capsule layer, the initial value of  $b_{ij}$  is 0 for capsule  $i$  in layer  $l$  and capsule  $j$  in layer  $(l+1)$ , as shown in (5).

$$b_{ij} \leftarrow b_{ij} + \hat{u}_{j|i} \cdot v_j \quad (5)$$

### D. Proposed method

As shown in figure.2. The specific implementation scheme is to obtain the EEG feature image of  $N$  (it turns on the frequency band energy features and eye-open states)  $\times 32 \times 32$  ( $32 * 32$  grid) as input and then passes through the standard convolutional layer, main capsule layer and digital capsule layer.

The first layer is the ordinary CNN layer, which acts as pixel-level local feature detection. The input is  $N \times 32 \times 32$  in size, and the first layer uses 256 convolutional  $9 \times 9$  cores with a stride of 1 and ReLU activation, resulting in an output matrix size of  $24 \times 24 \times 256$ .

The second layer is the main capsule layer (Primarycaps), which can be understood as a stack of 8 parallel conventional convolutional layers with  $8 \times 32$  convolution  $9 \times 9$  cores with a step size of 2, yielding 8 output matrices of  $8 \times 8 \times 1 \times 32$ , changing the 3 D output tensor  $6 \times 6 \times 1 \times 32$  under the traditional convolution to the 4 D output tensor  $6 \times 6 \times 8 \times 32$ , that is, each calculated output is a vector of length 8.

The third digital capsule layer (Digitcaps) spreads and routes updates based on the vector output of the second layer. The second layer outputs a total of  $8 \times 8 \times 32 = 2048$  vectors, each with a dimension of 8, namely, 2048 capsule units in layer  $i$ . While the third layer  $j$  has 2 standard capsule units, the output vector for each capsule has 16 elements. The number of capsule cells in the previous layer is 2048, so there will be  $2048 \times 2$  cells, each  $W_{ij}$  with dimensions of  $8 \times 16$ . When the predicted vectors are multiplied by their counterparts, we have  $2048 \times 2$  coupling coefficients  $c_{ij}$ , and the corresponding weighted sum yields 2 input vectors of  $16 \times 1$ . The input vector

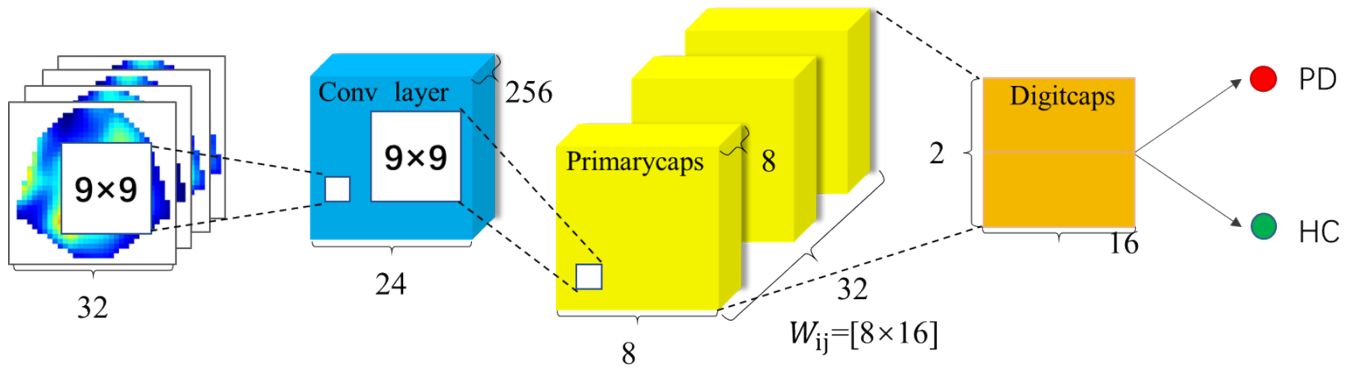


Figure 2. Overall structure of proposed method

Table. 2 The classification performance for different band inputs

feature	Accuracy	Sensitivity	Specificity
theta	82.49±3.07%	78.71±6.07%	86.28±6.22%
alpha	82.58±3.76%	78.40±4.40%	86.75±5.75%
beta	82.48±3.69%	75.84±3.21%	89.13±7.83%
gamma	83.85±4.76%	82.16±5.23%	85.54±8.05%
all	89.34±4.06%	86.88±4.10%	91.83±6.76%

Table. 3 The classification performance for different band inputs

feature	Accuracy	Sensitivity	Specificity
SVM	88.99±4.11%	86.45±7.14%	91.54±3.89%
CapsNet	89.34±4.06%	86.87±4.10%	91.83±6.76%

is input into the "squashing nonlinear function to obtain the final output vector, where the length indicates the probability of identification as a category.

### III Results & Discussion

In this study, we compared the CapsNet classification results with input among four bands, evaluated the contribution of different bands to the model. It suggests that the performance of the model classification increases with increasing frequency bands. As shown in Table 2, with a single band feature, we obtained a 5-fold cross-validated accuracy of 83.85% for the gamma band, 82.48% for the beta band, 82.58% for the alpha band and 82.49% for the theta band. It suggests that we need to pay more attention to the role of the gamma frequency band in Parkinson's pathology.

As shown in Table 3, we obtained a significant increase in accuracy of 89.34% for all band feature inputs (four frequency band energy features and two eye-open states). It has exceeded the classification accuracy of 88.99% on the same EEG with the multikernel SVM algorithm proposed by our team before [18].

### IV Conclusion

In this paper, we proposed a method to diagnose Parkinson's disease by EEG-based CapsNet. As a neural network model, this method has exceeded the classification accuracy of the SVM model in small samples (trained less than 100) and has the potential to identify Parkinson's disease electrophysiological signal characteristics and build a dynamic mapping model of Parkinson's disease patients, which can serve as an effective supplement to the current clinical Parkinson's diagnosis. Moreover, the good performance of the gamma band suggests that we need to value the role of the gamma frequency band in Parkinson's pathology.

### References

- [1] Lees A J, Hardy J, Revesz T. Parkinson's disease [J]. Lancet, 2009, 373(9680): 2055-66.
- [2] Poewe W, Seppi K, Tanner C M, et al. Parkinson disease [J]. Nat Rev Dis Primers, 2017, 3(21).

[3] Global, regional, and national burden of neurological disorders during 1990-2015: a systematic analysis for the Global Burden of Disease Study 2015. *GBD 2015*

[4] Neurological Disorders Collaborator Group. *Lancet Neurol.* 2017 Nov; 16(11):877-897.

[5] Ferrazzoli D, Carter A, Ustun FS, et al. Dopamine replacement therapy, learning and reward prediction in Parkinson's disease: implications for rehabilitation [J]. *Front Behav Neurosci*, 2016, 10(6): 121.

[6] Weingarten, C. P., Sundman, M. H., Hickey, P., & Chen, N. K. (2015). Neuroimaging of Parkinson's disease: Expanding views. *Neuroscience & Biobehavioral Reviews*, 59, 16-52.

[7] Tolosa, E., Wenning, G., Poewe, W., 2006. The diagnosis of Parkinson's disease. *Lancet Neurol.* 5, 75-86.

[8] Geraedts V J, Boon L I, Marinus J, et al. Clinical correlates of quantitative EEG in Parkinson disease A systematic review [J]. *Neurology*, 2018, 91(19): 871-83.

[9] 冀伟. 伴与不伴抑郁帕金森病患者脑电功率对比研究. *中国实用神经疾病杂志*[J]. 2014, 17(13): 47-9.

[10] Haynes W I A, Haber S N. The Organization of Prefrontal-Subthalamic Inputs in Primates Provides an Anatomical Substrate for Both Functional Specificity and Integration: Implications for Basal Ganglia Models and Deep Brain Stimulation [J]. *J Neurosci*, 2013, 33(11): 4804-14.

[11] Cavanagh J F, Figueroa C M, Cohen M X, et al. Frontal Theta Reflects Uncertainty and Unexpectedness during Exploration and Exploitation [J]. *Cereb Cortex*, 2012, 22(11): 2575-86.

[12] Georgiev D, Lange F, Seer C, et al. Movement-related potentials in Parkinson's disease [J]. *Clinical Neurophysiology*, 2016, 127(6): 2509-19.

[13] Bockova M, Rektor I. Impairment of brain functions in Parkinson's disease reflected by alterations in neural connectivity in EEG studies: A viewpoint [J]. *Clinical Neurophysiology*, 2019, 130(2): 239-47.

[14] Muslimovic D, Post B, Speelman J D, et al. Determinants of disability and quality of life in mild to moderate Parkinson disease [J]. 2008, 70(23): 2241-7.

[15] Mak M K, Wong-Yu I S, Shen X, et al. Long-term effects of exercise and physical therapy in people with Parkinson disease [J]. *Nat Rev Neurol*, 2017, 13(11): 689-703.

[16] BI, Xiaojun; WANG, Haibo. Early Alzheimer's disease diagnosis based on EEG spectral images using deep learning. *Neural Networks*, 2019, 114: 119-135.

[17] GEMEIN, Lukas AW, et al. Machine-learning-based diagnostics of EEG pathology. *NeuroImage*, 2020, 220: 117021.

[18] GUO, Guoxin. Diagnosing Parkinson's Disease Using Multimodal Physiological Signals. In: *Human Brain and Artificial Intelligence: Second International Workshop, HBAI 2020: Held in Conjunction with IJCAI-PRICAI 2020,*

Yokohama, Japan, January 7, 2021: Revised Selected Papers. Springer Nature, 2021. p. 125.

[19] Rim B, Sung N J, Min S, et al. Deep Learning in Physiological Signal Data: A Survey [J]. *Sensors (Basel, Switzerland)*, 2020, 20(4).

[20] SABOUR, Sara; FROSST, Nicholas; HINTON, Geoffrey E. Dynamic routing between capsules. *arXiv preprint arXiv:1710.09829*, 2017.

[21] BASHIVAN, Pouya, et al. Learning representations from EEG with deep recurrent-convolutional neural networks. *arXiv preprint arXiv:1511.06448*, 2015.